Inorg. Chem. **2004**, *43*, 6228–6237

Synthesis and Characterization of Novel Monocarbollide *exo-closo*-(π-Arene)biruthenacarboranes [$(PPh_3)_mClRu(\eta^6\text{-}C_6H_5R)Ru'CB_{10}H_{11-n}(OMe)_n$] (where R = H, m = 2, n = 1; R = μ-PPh_2, m = 1, n = 0, 1)

Irina V. Pisareva, Vitalii E. Konoplev, Pavel V. Petrovskii, Evgenii V. Vorontsov, Fedor M. Dolgushin, Alexandr I. Yanovsky, and Igor T. Chizhevsky*

A. N. Nesmeyanov Institute of Organoelement Compounds, Russian Academy of Sciences, 28 Vavilov Street, 119991 Moscow, Russian Federation

Received February 17, 2004

The monocarbon carborane [Cs][*nido*-7-$CB_{10}H_{13}$] reacts with the 16-electron [$RuCl_2(PPh_3)_3$] in a solution of benzene/methanol in the presence of *N*,*N*,*N*′,*N*′-tetramethylnaphthalene-1,8-diamine as the base to give a series of 12-vertex monocarbon arene-biruthenacarborane complexes of two types: [*closo*-2-{7,11-*exo*-$RuClPPh_3(\mu,\eta^6\text{-}C_6H_5PPh_2)$}-7,11-($\mu$-H)$_2$-2,1-$RuCB_{10}H_8R$] (**5**, R = H; **6**, R = 6-MeO; **7**, R = 3-MeO) and [*closo*-2-(η^6-C_6H_6)-10,11,12-{*exo*-$RuCl(PPh_3)_2$}-10,11,12-(μ-H)$_3$-2,1-$RuCB_{10}H_7R^1$] (**8a**, R^1 = 6-MeO; **8b**, R^1 = 3-MeO, inseparable mixture of isomers) along with trace amounts of 10-vertex mononuclear *hypercloso/isocloso*-type complexes [2,2-$(PPh_3)_2$-2-H-3,9-$(MeO)_2$-2,1-$RuCB_8H_7$] (**9**) and [2,5-(Ph_3P)-2-Cl-2-H-3,9-$(MeO)_2$-2,1-$RuCB_8H_6$] (**10**). Binuclear ruthenacarborane clusters of both series were characterized by a combination of analytical and multinuclear NMR spectroscopic data and by single-crystal X-ray diffraction studies of three selected complexes, **6**–**8**. In solution, isomers **8a**,**b** have been shown to undergo the isomerization process through the scrambling of the *exo*-{$RuCl(PPh_3)_2$} fragment about two adjacent triangular cage boron faces B(7)B(11)B(12) and B(8)B(9)B(12).

Introduction

The controlled basic degradation of icosahedral *closo*-metallacarboranes is probably the most widely known of the polyhedral contraction processes which lead to the intermediate and smaller cage metallacarborane systems.[1,2] Pursuing an alternative strategy, we and others have reported that 16-electron complexes [$RuCl_2(PPh_3)_3$] (**1**)[3,4] and [$OsCl_2(PPh_3)_3$][5] can promote polyhedral contraction reactions for some mono- and dicarbon *nido*- and *arachno*-carboranes. In particular, the reaction of **1** with the Cs^+ salt of the monocarbon carborane anion [*nido*-7-$CB_{10}H_{13}$]$^-$ (**2**) in methanol solution at a reflux temperature has been found to result in the formation of some smaller-cage ruthenacarboranes of {$RuCB_8$} and {$RuCB_6$} cluster structure.[3] More recently, we have reported that ruthenium complex **1** in the reaction with a neutral carborane [*nido*-5,6-$C_2B_8H_{12}$] (**3**) in hot toluene effected the polyhedral contraction of **3** to form the 7-vertex ruthenacarborane [*closo*-1,1-$(PPh_3)_2$-1-H-1-Cl-1,2,3-$RuC_2B_4H_6$] (**4**) as the principal product.[6] In fact, since all of these transformations did not occur under basic conditions but at rather moderate temperatures, one may reasonably conclude that the 16-electron complexes could serve in the reactions both as degrading and coordinating agents and as reagents promoting the loss of bridging hydrogen atoms from the original *nido*- and/or *arachno*-carboranes.[3−6] However, if starting carborane **3** was deprotonated with the *N*,*N*,*N*′,*N*′-

* Author to whom correspondence should be addressed. E-mail: chizbor@ineos.ac.ru.

(1) Callahan, K. P.; Hawthorne, M. F. *Adv. Organomet. Chem*. **1976**, 145.
(2) Hanusa, T. P.; Huffman, J. C.; Curtis, T. L.; Todd, L. J. *Inorg. Chem.* **1985**, *24*, 787.
(3) (a) Pisareva, I. V.; Chizhevsky, I. T.; Petrovskii, P. V.; Bregadze, V. I.; Dolgushin, F. M.; Yanovsky, A. I. *Organometallics* **1997**, *16*, 5598. (b) Pisareva, I. V.; Dolgushin, F. M.; Yanovsky, A. I.; Balagurova, E. V.; Petrovskii, P. V.; Chizhevsky, I. T. *Inorg. Chem*. **2001**, *40*, 5318.
(4) (a) Teixidor, F.; Viñas, C.; Casabó, J.; Romerosa, A. M.; Rius, J.; Miravitlles, C. *Organometallics* **1994**, *13*, 914. (b) Teixidor, F.; Viñas, C.; Abad, M. M.; Lopes, M.; Casabó, J. *Organometallics* **1993**, *12*, 3766. (c) Teixidor, F.; Benakki, R.; Viñas, C.; Kivekäs, R.; Sillanpää, R. *Organometallics* **1998**, *17*, 4630. (d) Viñas, C.; Abad, M. M.; Teixidor, F.; Sillanpää, R.; Kivekäs, R. *J. Organomet. Chem*. **1998**, *555*, 17.
(5) Konoplev, V. E.; Pisareva, I. V.; Vorontsov, E. V.; Dolgushin, F. M.; Franken, A.; Kennedy, J. D.; Chizhevsky, I. T. *Inorg. Chem. Commun.* **2003**, *6*, 1454.

10.1021/ic0497883 CCC: $27.50
Published on Web 08/26/2004

Scheme 1

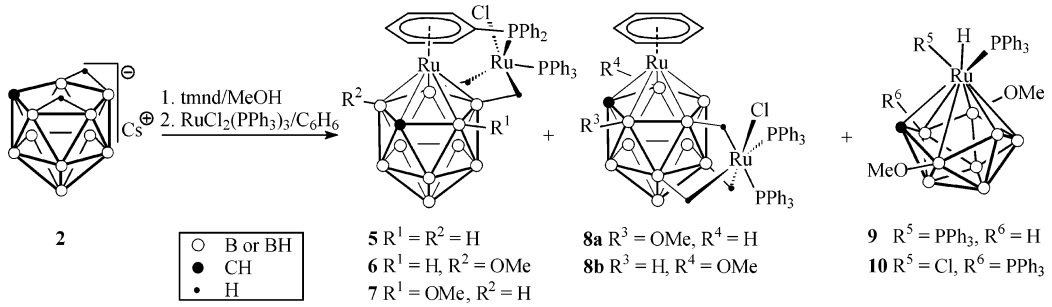

2

5 $R^1 = R^2 = H$
6 $R^1 = H$, $R^2 = OMe$
7 $R^1 = OMe$, $R^2 = H$

8a $R^3 = OMe$, $R^4 = H$
8b $R^3 = H$, $R^4 = OMe$

9 $R^5 = PPh_3$, $R^6 = H$
10 $R^5 = Cl$, $R^6 = PPh_3$

tetramethylnaphthalene-1,8-diamine prior to its use (the nonnucleophilic base which is frequently used for the abstraction of the bridging protons from the polyhedral boranes and carboranes,[7] abbreviated below as tmnd) and then reacted with complex **1** in hot arene solvents, a series of 11-vertex arene-ruthenium complexes [*isonido*-1-(η^6-arene)-3(6)-Cl-1,2,4-$RuC_2B_8H_9$] (arene = C_6H_6, 1,4-$Me_2C_6H_4$, MePh, etc.) were produced, along with only a small amount of complex **4**.[8] Looking for other examples of metal-promoted polyhedral contraction processes which may proceed in different ways, depending on whether *nido*-carborane or its deprotonated congener is employed as the starting reagent, we have examined in the present work the reaction of complex **1** with the trianion [*nido*-7-$CB_{10}H_{11}]^{3-}$ (assumed to be formed in situ during the treatment of **2** with tmnd).

We have found that the earlier observed reaction pathway[3] dramatically changes if **1** and **2** are heated in a MeOH/C_6H_6 mixture in the presence of 2 equiv of tmnd. This results (Scheme 1) in the formation of a number of novel monocarbon *exo-closo*-(η^6-arene)biruthenacarborane complexes, **5**−**7** and **8a,b** (inseparable mixture of two positional isomers), in which one metal atom is ligated by the open CB_4 face of the *nido*-{7-CB_{10}} cage in a η^5-coordination mode forming a *closo*-{2,1-$RuCB_{10}$} framework, while the other is bound exopolyhedrally to the cage framework via two or three B−H···Ru linkages, depending on whether the μ,η^6-arene- or the η^6-arene-to-metal coordination mode occurs. In addition, the earlier reported[3a] mononuclear 10-vertex ruthenacarboranes **9** and **10** have been isolated from the reaction mixture in trace quantities.

Herein, we report the results of this study, focusing mainly on the solution and solid-state structural examination of the novel bimetallacarborane clusters obtained.

Results and Discussion

Synthesis and Spectroscopic Characterization of *exo-closo*-(η^6-Arene)biruthenacarboranes 5−8 and Mononuclear Complexes 9 and 10. When monocarbon *nido*-carborane **2** was treated with a 2-fold excess of tmnd in methanol and 2 equiv of **1** and heated in a benzene/methanol mixture for 4 h, metallacarborane products **5**−**10** were formed in yields of ca. 42% (total content). Each of these has been successfully isolated as an air-stable crystalline solid by repeated column chromatography on silica gel.

Due to the very poor solubility of starting complex **1** in methanol, on one hand, and the Cs^+ salt of *nido*-carborane **2** in benzene, on the other, we had to run the reaction in the mixture of the above solvents in a 1:1 ratio. This allowed us to maintain more or less homogeneous reaction conditions. Our attempts to carry out the reaction in heterogeneous conditions using either benzene or methanol as the only solvent were much less successful. This, in the case of benzene, led to the substantial decomposition of **1** with the precipitation of dark intractable materials during the heating of the reaction mixture. In the case of methanol, the reaction rates and total yields of products **5**−**10** were dramatically decreased, and no selectivity in the formation of any products was observed.

The bimetallic species thus isolated, on the basis of multinuclear NMR spectral data, may be categorized in two different families. The first group involves complexes [*closo*-2-{7,11-*exo*-$RuClPPh_3(\mu,\eta^6$-$C_6H_5PPh_2)$}-7,11-(μ-H)$_2$-2,1-$RuCB_{10}H_8R$] (**5**, R = H; **6**, R = 6-MeO; **7**, R = 3-MeO), where one of the phenyl rings of one triphenylphosphine ligand at the exopolyhedral ruthenium center functions as an η^6-arene ligand to the second ruthenium atom giving rise to a classical 12-vertex monocarbon *closo*-metallacarborane unit, which, in turn, is connected with the exopolyhedral ruthenium-containing moiety, {$RuCl(PPh_3)(\mu,\eta^6$-$C_6H_5PPh_2)$}, via two three-center two-electron (3c, 2e) B−H···Ru bonds. Bimetallic complexes [*closo*-2-(η^6-C_6H_6)-10,11,12-{*exo*-$RuCl(PPh_3)_2$}-10,11,12-(μ-H)$_3$-2,1-$RuCB_{10}H_7R^1$], which are formed as an inseparable mixture of positional isomers **(8a**, R^1 = 6-MeO; **8b**, R^1 = 3-MeO) in a ratio of ca. 3.7:1, respectively, belong to the second family, where the {$RuCl(PPh_3)_2$}$^+$ moiety is exopolyhedrally attached to the discrete monocarbon *closo*-(η^6-benzene)ruthenacarborane framework via three 3c, 2e B−H···Ru bridging bonds. In addition, using the column chromatography of the crude reaction mixture, we were also able to isolate in trace quantities two known[3a] mononuclear complexes **9** and **10**, which are formed in the reaction, presumably, due to the metal-promoted polyhedral

(6) Pisareva, I. V.; Dolgushin, F. M.; Tok, O. L.; Konoplev, V. E.; Suponitsky, K. Yu.; Yanovsky, A. I.; Chizhevsky, I. T. *Organometallics* **2001**, *20*, 4216.

(7) See for instance: (a) Greenwood, N. N.; Kennedy, J. D.; Thornton-Pett, M.; Woollins, J. D. *J. Chem. Soc., Dalton Trans.* **1985**, 2397. (b) Fontaine, X. L. R.; Greenwood, N. N.; Kennedy, J. D.; MacKinnon, P. *J. Chem. Soc., Dalton Trans.* **1988**, 1785. (c) Bown, M.; Fontaine, X. L. R.; Greenwood, N. N.; Kennedy, J. D.; Thornton-Pett, M. *J. Chem. Soc., Dalton Trans.* **1990**, 3039. (d) Bown, M.; Gruner, B.; Stibr, B.; Fontaine, X. L. R.; Thornton-Pett, M.; Kennedy, J. D. *J. Organomet. Chem.* **2000**, *614*−*615*, 269.

(8) Konoplev, V. E.; Pisareva, I. V.; Lemenovskii, D. A.; Petrovskii, P. V.; Tok, O. L.; Dolgushin, F. M.; Chizhevsky, I. T. *Collect. Czech. Chem. Commun.* **2002**, *67*, 936.

Table 1. ^{1}H, ^{31}P, and ^{11}B NMR Data of Complexes **5**−**7**[a]

	$^{1}H/\delta$[b]	$^{31}P/\delta$	$^{11}B/\delta$
5	8.77 (t, 1H, H(5), $J_t = 6.1$), 7.64−7.16, 6.82 (m, 23H + 2H, H_{Ph}), 6.36 (t, 1H, H(4), $J_t = 6.1$), 5.95 (t, 1H, H(3), $J_t = 5.9$), 5.64 (t, 1H, H(2), $J_t = 6.1$), 4.55 (t, 1H, H(1), $J_t = 6.5$), 3.30 (s br, 1H, CH_{Cb}), −0.14 (m br, 1H, BH), −16.56 m (br, 1H, BH)	68.8, 65.1 (d, each 1P, P,[a] P,[b] $J = 36$)	10.4 (s br, 1B), 9.5 (s br, 1B), −2.7 (s br, 1B), −4.6 (s br, 1B), −7.3 (s br, 1B), −8.8 (d br, 1B, 117), −18.6 (d br, 4B, 112)
6	8.85 (t, 1H, H(5), $J_t = 6.3$), 7.61−7.10, 6.78 (m, 23H + 2H, H_{Ph}), 6.09 (t, 1H, H(4), $J_t = 6.3$), 6.03 (t, 1H, H(3), $J_t = 6.1$), 5.74 (t, 1H, H(2), $J_t = 6.1$), 4.40 (t, 1H, H(1), $J_t = 6.5$), 3.62 (s br, 1H, CH_{Cb}), 3.45 (s, 3H, MeO), 0.36 (m br, 1H, BH), −16.66 (m br, 1H, BH)	69.2, 64.7 (d, each 1P, P,[a] P,[b] $J = 35$)	19.3 (s br, 1B, B−OMe), 9.9 (s br, 1B), 6.5 (d br, 1B, 142), −6.3 (s br, 1B), −8.8 (d br, 1B, 112), −11.3 (d br, 1B, 117), −18.2 (d br, 1B, 112), −19.1 (s br, 1B), −20.3 (d br, 1B, 142), −24.1 (d br, 1B, 137)
7	8.48 (t, 1H, H(5), $J_t = 5.9$), 7.62−7.14, 6.87 (m, 23H + 2H, H_{Ph}), 6.19 (t, 1H, H(4), $J_t = 6.4$), 6.00 (t, 1H, H(3), $J_t = 5.9$), 5.70 (t, 1H, H(2), $J_t = 6.2$), 4.32 (t, 1H, H(1), $J_t = 6.4$), 3.61 (s br, 1H, CH_{Cb}), 3.15 (s, 3H, MeO), −0.48 (m br, 1H, BH), −16.23 (m br, 1H, BH)	65.8, 65.3 (d, each 1P, P,[a] P,[b] $J = 35$)	17.2 (s br, 1B, B−OMe), 7.8 (s br, 1B), 5.8 (d br, 1B, 107), −4.0 (s br, 1B), −7.8 (d br, 1B, 148), −10.3 (d br, 1B, 108), −17.0 (d br, 1B, 157), −19.8 (s br, 1B), −21.1 (d br, 1B, 142), −24.6 (d br, 1B, 130)

[a] Chemical shifts in parts per million, coupling constants in hertz, and measurements in CD_2Cl_2 at room temperature. [b] The assignment of aromatic H(1)−H(5) signals was made by selective proton decoupling experiments (see Supporting Information).

contraction of starting carborane **2**; the ^{1}H, ^{31}P, and ^{11}B NMR spectroscopic data for **9** and **10** are consistent with those of authentic samples.

The ^{1}H NMR spectra of all arene-biruthenacarborane species show some similarities in that they all display a set of broad high-field resonances, diagnostic of the presence of B−H···Ru groups, and resonances characteristic of arene ligands bound to one of the Ru atoms in an η^6-coordination mode. However, the mixture of isomeric complexes **8a**,**b** displayed two principal arene singlets at δ 5.52 and 5.50 ppm in the ^{1}H NMR spectrum (see below), whereas the spectra of complexes **5**−**7**, by contrast, contained a set of five well-defined arene multiplets, each corresponding to one proton via integration. These latter peaks appear to originate from the monosubstituted phenyl rings functioning as μ,η^6-coordinating ligands between the phosphorus atom of one of the triphenylphosphine groups attached to the *exo*-Ru atom and the other Ru atom incorporated as a vertex in the *closo*-metallacarborane framework. These aromatic resonances in the case of **5**, taken as an example, were assigned as such on the basis of selective proton decoupling experiments (see Supporting Information). The relevant details are listed in the Table 1, with the assignments made by analogy to two other related species **6** and **7**. In addition, the ^{1}H NMR spectra of both **6** and **7** each show singlet resonances at δ 3.45 and 3.15 ppm of the relative intensity area of 3H, respectively, and were assigned, therefore, to the cage-bound methoxy groups. In agreement with this are the proton-coupled ^{11}B NMR spectra of **6** and **7**, where only one singlet resonance from a set of doublets was observed for each of these complexes. Provided that the exopolyhedral {RuCl(PPh$_3$)(μ,η^6-PhPPh$_2$)} moiety in **6** and **7** each retains a similar ligand orientation with regard to the *exo*-Ru center, these species can be best formulated as isomers that differ by the position of the cage boron atoms to which the methoxy groups are attached. An interesting feature of the ^{1}H NMR spectra of **5**−**7** is that of the two *ortho*-hydrogen resonances, derived from a bridging μ,η^6-phenyl ligand, one is considerably shifted downfield and is observed in the region from δ 8.5 to 9.0 ppm, whereas the other four aromatic peaks span the range typical for η^6-coordinating arene moieties. Such a strong deshielding of the phenyl *ortho*-hydrogen resonances in **5**−**7** is indicative of their high protonic character caused by the presence of a specific inter- or intramolecular interaction in which they are involved. It has further been proven to be the case by the analysis of the X-ray structures of complexes **6** and **7**, where the existence of an intramolecular hydrogen-bonding Ph-*ortho*-H···Cl interaction was revealed (vide infra).

The examination of the $^{31}P\{^{1}H\}$ and $^{11}B/^{11}B\{^{1}H\}$ NMR spectra of complexes **5**−**8** provided additional information regarding their structures. The $^{31}P\{^{1}H\}$ NMR spectra of **5**−**7** each display two separate doublets with a ^{2}J(P,P) coupling in the range of 35−36 Hz originating from the nonequivalent PPh$_3$ ligands (Table 1), as expected for molecules lacking mirror symmetry. The $^{31}P\{^{1}H\}$ NMR spectrum of the mixture of isomers **8a**,**b** proved, however, to be more complicated, displaying, along with the two principal broad resonances at δ 58.6 and 53.7 ppm, a set of partly overlapping weak resonances that might be consistent with the presence of at least several conformationally different species in solution, a feature that will be discussed in detail below.

Although a number of bonding details of bimetallic complexes **5**−**8** were obtained from the ^{1}H and ^{31}P NMR studies, these complex molecular structures and, especially, stereochemical peculiarities of **6** and **7**, on one hand, and the isomerism found in **8a**,**b**, on the other, could not be fully deduced from the spectroscopic data alone. Therefore, the two isomeric complexes **6** and **7**, as well as complex **8**, were the subjects of single-crystal X-ray diffraction studies (see below).

Single-Crystal X-ray Diffraction Studies of Complexes 6 and 7. Each of complexes **6** and **7** has two independent molecules which show only small differences in their bond distances and angles (selected values are listed in Table 2), and the molecular structure of only one of them in each case is therefore shown in Figure 1.

The overall geometry of **6** and **7** confirmed clearly that they are positional isomers in which a methoxy group is attached to the cage B(6) and B(3) atoms, respectively, lying

Table 2. Selected Geometrical Parameters for Two Independent Molecules in Complexes **6** and **7**

	6		**7**	
	A	B	A	B
	Bond Lengths (Å)			
Ru(1)−Ru(2)	2.9774(7)	3.0128(7)	2.948(1)	2.988(1)
Ru(1)−Cl(1)	2.408(1)	2.405(1)	2.395(2)	2.403(2)
Ru(1)−P(1)	2.203(2)	2.201(2)	2.213(2)	2.203(2)
Ru(1)−P(2)	2.255(2)	2.256(2)	2.262(2)	2.258(2)
Ru(1)−B(7)	2.189(7)	2.190(7)	2.204(7)	2.206(7)
Ru(1)−B(11)	2.538(6)	2.581(6)	2.458(7)	2.492(7)
Ru(1)−H(7)	1.57(5)	1.61(5)	1.60(6)	1.61(7)
Ru(1)−H(11)	2.31(5)	2.46(6)	2.14(7)	2.34(6)
Ru(2)−C(1)	2.160(6)	2.148(5)	2.154(7)	2.157(6)
Ru(2)−B(3)	2.194(6)	2.188(6)	2.200(7)	2.196(7)
Ru(2)−B(6)	2.222(7)	2.204(6)	2.201(7)	2.215(7)
Ru(2)−B(7)	2.227(7)	2.212(6)	2.220(7)	2.208(6)
Ru(2)−B(11)	2.247(6)	2.227(6)	2.255(7)	2.264(6)
Ru(2)−C(14)	2.240(5)	2.236(5)	2.262(6)	2.256(6)
Ru(2)−C(15)	2.255(5)	2.252(5)	2.254(6)	2.251(6)
Ru(2)−C(16)	2.252(5)	2.240(5)	2.248(6)	2.235(6)
Ru(2)−C(17)	2.231(5)	2.238(5)	2.270(6)	2.260(6)
Ru(2)−C(18)	2.275(5)	2.276(5)	2.315(6)	2.293(6)
Ru(2)−C(19)	2.263(5)	2.259(5)	2.266(6)	2.267(6)
P(1)−C(14)	1.833(6)	1.836(6)	1.844(6)	1.843(6)
P(1)−C(20)	1.811(6)	1.816(6)	1.819(6)	1.818(6)
P(1)−C(26)	1.828(6)	1.826(6)	1.823(6)	1.827(6)
O(1)−B(6)	1.407(8)	1.412(7)		
O(1)−B(3)			1.405(9)	1.396(8)
O(1)−C(13)	1.414(6)	1.420(6)	1.383(10)	1.413(8)
	Bond Angles (deg)			
P(1)−Ru(1)−Cl(1)	97.15(6)	97.73(5)	93.51(7)	94.02(7)
P(2)−Ru(1)−Cl(1)	90.41(5)	93.60(5)	90.30(7)	91.96(7)
P(1)−Ru(1)−P(2)	105.24(6)	103.29(6)	105.71(6)	105.00(7)
H(7)−Ru(1)−Cl(1)	177(1)	172(1)	174(2)	175(2)
H(7)−Ru(1)−P(1)	83(1)	90(1)	86(2)	91(2)
H(7)−Ru(1)−P(2)	87(1)	83(1)	96(2)	87(2)
H(7)−Ru(1)−H(11)	101(2)	99(2)	100(4)	97(4)
Cl(1)−Ru(1)−H(11)	81(1)	77(1)	76(2)	79(2)
P(1)−Ru(1)−H(11)	140(1)	137(1)	143(2)	139(2)
P(2)−Ru(1)−H(11)	115(1)	120(1)	110(2)	116(2)
Cl(1)−Ru(1)−Ru(2)	106.40(4)	106.20(4)	106.36(5)	107.86(5)
P(1)−Ru(1)−Ru(2)	79.35(4)	78.33(4)	81.68(6)	80.96(5)
P(2)−Ru(1)−Ru(2)	162.05(4)	159.82(4)	161.52(4)	159.02(4)
H(7)−Ru(1)−Ru(2)	76(1)	77(1)	67(1)	72(1)
H(11)−Ru(1)−Ru(2)	63(1)	63(1)	68(1)	63(1)
C(20)−P(1)−C(14)	106.9(3)	106.5(3)	108.2(3)	107.5(3)
C(26)−P(1)−C(14)	103.2(3)	103.4(3)	103.2(3)	104.1(3)
C(20)−P(1)−C(26)	99.8(3)	100.2(3)	102.8(3)	102.6(3)
C(14)−P(1)−Ru(1)	93.6(2)	94.6(2)	91.2(2)	92.1(2)
C(20)−P(1)−Ru(1)	125.5(2)	125.1(2)	123.2(2)	123.1(2)
C(26)−P(1)−Ru(1)	124.2(2)	123.7(2)	124.5(2)	124.0(2)
B(6)−O(1)−C(13)	119.9(5)	119.7(5)		
B(3)−O(1)−C(13)			125.3(7)	120.0(5)

either in the *anti* or *syn* position with respect to the Cl ligand on the cage-bound *exo*-Ru(1) atom. This Ru(1) atom in both structures is also involved in the coordination with two triphenylphosphine ligands forming an *exo*-{RuCl(PPh_3)-(PPh_2-μ,η^6-C_6H_5)}$^+$ fragment which interacts with two B(7)−H and B(11)−H bonds, thus involving both β-boron atoms in the upper pentagonal {CB_4} belt with respect to the cage carbon atom. Atom Ru(2) in both species **6** and **7** is η^5-coordinated by the {CB_4} plane of the carborane ligand and, in addition, η^6-coordinated by the phenyl ring belonging to one of the triphenylphosphine ligands at the *exo*-Ru(1) atom. Such a μ,η^6-coordination mode of triphenylphosphine ligands in bi- or polynuclear complexes has a number of precedents in organometallic chemistry.[9] However, we are aware of only one crystallographically studied species of this type among the polyhedral boron-based mixed-metal complexes, [(PMe_2Ph)$_2$-μ,η^6(Ru)-η^1(Pt)-($C_6H_5PPh_2$)-*closo*-$PtRuB_9H_9$],[10] in which a PPh_3 ligand on one metal atom (Pt) acts as an η^6-coordinating ligand toward another metal atom (Ru).

Of particular interest is the coordination geometry of the cage-bound *exo*-Ru(1) atom, as determined in structures **6** and **7**. The separation between the two Ru(1) and Ru(2) metals found in each of the independent molecules of **6** and **7** (average distances are 2.995 and 2.968 Å, respectively) is at the higher end of the reported Ru−Ru bonding distances[11] and, in this respect, may be compared with that found in [*closo*-3-{*exo*-(3,8-μ,σ-Ru(CO)$_3$$PPh_3$)}-($\mu$-H)-3-CO-3-$PPh_3$-3,1,2-$RuC_2B_9H_{10}$] (2.9356 Å)[12] and even in [Et_4N][*closo*-3,3′-(CO)$_2$-3,3′-(μ-H)-3,1,2-$RuC_2B_9H_{11}$]$_2$ (3.189 Å),[13] where the existence of a metal−metal interaction has been considered. Thus, the above Ru−Ru separation found in **6** and **7** might also be interpreted as an indication of the existence of a single metal−metal bond. Considered in this way, the *exo*-Ru(1) atom in complexes **5**−**7** possesses a coordination number of six, while the Ru(2) atom would then be seven-coordinate, assuming the η^5-carbollide and η^6-arene ligands each occupy three facial coordination sites and the metal−metal bond is included. However, no structural precedents are available, to our knowledge, for mono- or binuclear 12-vertex platinum metal *closo*-metallacarborane species in which a d^6 metal vertex involved in π-coordination with a planar carbocyclic ligand would be seven-coordinate.

Analysis of the Ru(1) coordination geometry in **6** and **7** appears, however, to give more convincing evidence for the alternative bonding description of these molecules, which implies the absence of a metal−metal interaction and allows one to consider these molecules as zwitterionic species formally built from a cationic 12-electron *exo*-{Ru(1)Cl-(PPh_3)(PPh_2-μ,η^6-C_6H_5)}$^+$ fragment supplemented by the two exopolyhedral B−H···Ru bonds and the 18-electron anion {*closo*-(η^6-C_6H_5R)Ru(2)CB_{10}}$^-$ (where R represents a Ru(1)-bound PPh_2 group). As can be seen from the selected structural data listed in Table 1, an octahedral coordination of Ru(1), which would be expected in the presence of a metal−metal bond, proved to be noticeably distorted. Most of the *cis* and *trans* angles around the Ru(1) atom [i.e., *cis*-P(1)−Ru(1)−P(2), *cis*-Cl(1)−Ru(1)−Ru(2), *cis*-P(1)−Ru(1)−Ru(2), and *trans*-P(2)−Ru(1)−Ru(2)] are significantly higher or lower than the standard values (90 and/or 180°). Thus, it could be argued that the close approach between

(9) See for instance: (a) Luck, R.; Morris, R. H.; Sawyer, J. F. *Organometallics* **1984**, *3*, 1009. (b) Eischenbroich, C.; Isenburg, T.; Metz, B.; Behrendt, A.; Harms, K. *J. Organomet. Chem.* **1994**, *481*, 153. (c) Hsu, H.-Fu.; Wilson, S. R.; Shapley, J. R. *Organometallics* **1997**, *16*, 4937. (d) Marcazzan, P.; Ezhova, M. B.; Patrick, B. O.; James, B. R. *C. R. Chem.* **2002**, *5*, 373.

(10) Kim, Y.-H.; McKinnes, Y. M.; Cooke, P. A.; Greatrex, R.; Kennedy, J. D.; Thornton-Pett, M. *Collect. Czech. Chem. Commun.* **1999**, *64*, 938.

(11) See for instance: (a) Howard, J.; Woodward, P. *J. Chem. Soc., Dalton Trans.* **1975**, 59. (b) Churchill, M. R.; DeBoer, B. G.; Rotella, F. J. *Inorg. Chem.* **1976**, *15*, 1843. (c) Mattson, B. M.; Heiman, J. R.; Pignolet, L. H. *Inorg. Chem.* **1976**, *15*, 564 and references therein.

(12) Ellis, D. D.; Couchman, S. M.; Jeffery, J. C.; Malget, J. M.; Stone, F. G. A. *Inorg. Chem.* **1999**, *38*, 2981.

(13) Anderson, S.; Mullica, D. F.; Sappenfield, E. L.; Stone, F. G. A. *Organometallics* **1995**, *14*, 3516.

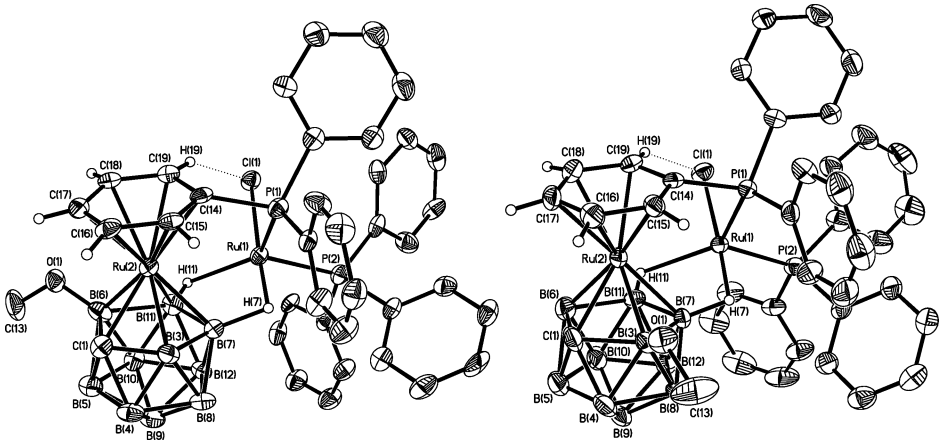

Figure 1. ORTEP representation of the molecular structures of complexes **6** (left) and **7** (right) with thermal ellipsoids at the 50% probability level. Hydrogen atoms, except for H(7), H(11), and H(19) (involved in the B−H···Ru and C(Ph-*o*)-H···Cl bonding interactions), have been omitted for clarity.

these two metal atoms is the result of conformational rigidity caused by the η^6-coordination of one of the phenyl rings of a triphenylphosphine moiety to the Ru(2) vertex, and the Ru(1) atom is actually five-coordinate. Indeed, the coordination geometry around the Ru(1) center seems to be better described in terms of a distorted trigonal bipyramid (TBP), where the equatorial triangular plane is formed by the P(1), P(2), and H(11) centers; axial Cl and H(7) atoms lie nearly perpendicular to this plane, and the Cl−Ru−H(7) angle is ca. 175° (for complexes **6** and **7**). However, while the Ru(1) atom in both structures **6** and **7** lies almost in the equatorial P(1)P(2)H(11) plane (within 0.08 Å), a trigonal geometry of this plane is marginally distorted from an idealized to a Y-shaped geometry, with average angles of 117.5 and 113° for H(11)−Ru(1)−P(2), 138.5 and 141° for P(1)−Ru(1)−H(11), and 104.3 and 105.35° for P(1)−Ru(1)−P(2) for **6** and **7**, respectively. Despite quite reasonable values observed for the former angles, the other two angles within the equatorial plane differed noticeably from the ideal value of 120°. It should, however, be noted that many other known five-coordinate phosphine-containing d^6 complexes with a Y-shape distorted TBP geometry display an analogous trend in the deviation of the equatorial angles.[14] Within this model, one would suggest that an interaction between the two metals in **5**−**7** can, in principle, be achieved through the formation of a donor−acceptor Ru(2) → Ru(1) bond[15] that would allow an 18-electron valence shell to exist on the Ru(1) atom.

In both structures **6** and **7**, the Ru(2)−C(1) bond distances (2.154 Å for **6** and 2.156 Å for **7**) are noticeably shorter than those between Ru(2) and four other boron atoms in the pentagonal CB_4 open face (average distances of 2.215 and 2.220 Å for **6** and **7**, respectively). These may, for example, be compared with the metal-to-carbon (2.198 and 2.143 Å) and metal-to-boron (2.172 and 2.075 Å) bond distances found, respectively, in the crystallographically studied arene-metal monocarbon metallacarboranes [*closo*-2-(η^6-C_6H_5Me)-1-($(Me_3Si)_2CH$)-2,1-$CoCB_{10}H_{10}$][16] and [*closo*-2-(η^6-$C_6H_3Me_3$-1,3,5)-1-$NHBu^t$-2,1-$RhCB_{10}H_{10}$],[17] where they are, however, inverted. The upper CB_4 pentagonal face of the carborane cage in both **6** and **7** is characteristically[18] folded about the B(3)···B(6) line, giving rise to folding angles of 6.4 and 8.0°, and 6.1 and 7.8°, respectively.

A particularly noteworthy structural feature of **6** and **7** is the existence of an intramolecular Ph-*ortho*-H···Cl hydrogen bond, as has been predicted on the basis of their ^{1}H NMR data. The very close approach of the *ortho*-phenyl carbon atom C(19) and the related hydrogen atom H(19) to the chlorine ligand established in **6** and **7** [averaged distances are 3.295 Å for C(19)···Cl and 2.40 Å for H(19)···Cl], coupled with the value of the C(19)−H···Cl angle of 149° observed in **6** and **7**, clearly confirmed the presence of such a specific intramolecular interaction in these molecules.

Single-Crystal Structure and Solution Behavior of Complex 8. A tridentate *exo* coordination mode of *nido*-[19] and *closo*-carboranes,[20] polyhedral boranes,[21] and icosahedral *closo*-metallacarboranes[22] to the cationic metal-containing groups via bridging B−H···M linkages is, at present, well documented. However, of the dozen or so "three-bridge"

(14) (a) Hughes, D. L.; Pombeiro, A. J. L.; Pickett, C. J.; Richards, R. L. *J. Organomet. Chem.* **1983**, *248*, C26. (b) Mezzetti, A.; Zotto, A. D.; Rigo, P. *J. Chem. Soc., Dalton Trans.* **1989**, 1045. (c) Chin, B.; Lough, A. J.; Morris, R. H.; Schweitzer, C. T.; D'Agostino, C. *Inorg. Chem.* **1994**, *33*, 6278.

(15) Astier, A.; Daran, J.-C.; Jeannin, Y.; Rigault, C. *J. Organomet. Chem.* **1983**, *241*, 53.

(16) Quintana, W.; Ernest, R. L.; Carroll, P. J.; Sneddon, L. G. *Organometallics* **1988**, *7*, 166.

(17) Jeffery, J. C.; Jelliss, P. A.; Lebedev, V. N.; Stone, F. G. A. *Organometallics* **1996**, *15*, 4737.

(18) (a) Carroll, W. E.; Green, M.; Stone, F. G. A.; Welch, A. J. *J. Chem. Soc., Dalton Trans.* **1975**, 2263. (b) Chizhevsky, I. T.; Pisareva, I. V.; Petrovskii, P. V.; Bregadze, V. I.; Yanovsky, A. I.; Struchkov, Yu. T.; Knobler, C. D.; Hawthorne, M. F. *Inorg. Chem.* **1993**, *32*, 3393. (c) Lebedev, V. N.; Mullica, D. F.; Sappenfield, E. L.; Stone, F. G. A. *Organometallics* **1996**, *15*, 1669. (d) Pisareva, I. V.; Chizhevsky, I. T.; Petrovskii, P. V.; Vorontzov, E. V.; Bregadze, V. I.; Dolgushin, F. M.; Yanovsky, A. I. *Inorg. Chim. Acta* **1998**, *280*, 233.

(19) (a) Chizhevsky, I. T.; Lobanova, I. A.; Bregadze, V. I.; Petrovskii, P. V.; Antonovich, V. A.; Polyakov, A. V.; Yanovsky, A. I.; Struchkov, Yu. T. *Mendeleev Commun.* **1991**, 48. (b) Lobanova, I. A.; Bregadze, V. I.; Timofeev, S. V.; Petrovskii, P. V.; Starikova, Z. A.; Dolgushin, F. M. *J. Organomet. Chem.* **2000**, *597*, 48. (c) Kolomnikova, G. D.; Sorokin, P. V.; Chizhevsky, I. T.; Petrovskii, P. V.; Bregadze, V. I.; Dolgushin, F. M.; Yanovsky, A. I. *Russ. Chem. Bull.* **1997**, *46*, 1971 (English translation). (d) Kolomnikova, G. D.; Petrovskii, P. V.; Sorokin, P. V.; Dolgushin, F. M.; Yanovsky, A. I.; Chizhevsky, I. T. *Russ. Chem. Bull.* **2001**, *50*, 706 (English translation).

(20) Crowther, D. J.; Borowski, S. I.; Swenson, D.; Meyer, T. Y.; Jordan, R. F. *Organometallics* **1993**, *12*, 2897.

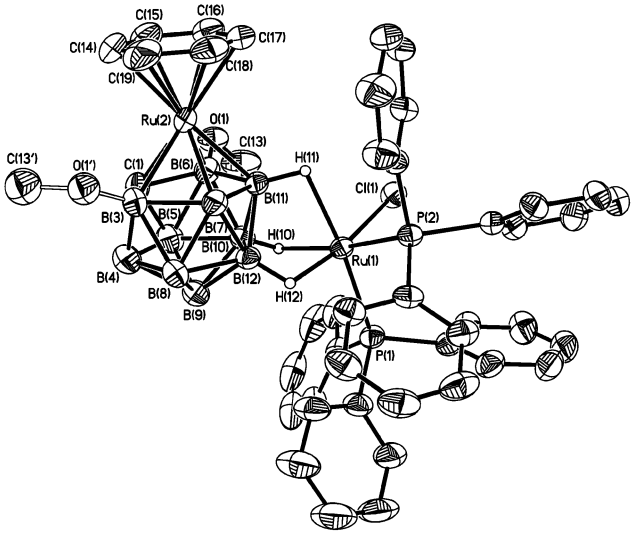

Figure 2. ORTEP representation of the molecular structure of complex **8** with thermal ellipsoids at the 50% probability level, showing both methoxy substituents disordered over the B(6) and B(3) atoms. Hydrogen atoms, except for H(10), H(11), and H(12) (involved in the B−H···Ru bonding interaction), have been omitted for clarity.

monometallic *exo-nido*- and bimetallic *exo-closo*-metallacarborane species reported so far, structurally characterized species based on the monocarbon metallacarborane framework are limited. As far as we are aware, there are only two examples, [*closo*-2,2,2-$(CO)_3$-2-PPh_3-*exo*-7,8,12-$(CuPPh_3)$-7,8,12-$(\mu$-H$)_3$-2,1-$MoCB_{10}H_8$] and [*closo*-2,2,2-$(CO)_3$-2-PPh_3-*exo*-7,8,12-{$RuCl(PPh_3)_2$}-7,8,12-$(\mu$-H$)_3$-2,1-$MoCB_{10}H_8$] (**11**), recently reported by Stone and coworkers.[22e] With this in mind, of special interest in this work was the determination of the solid-state structure of **8**, the first homometallic monocarbon *exo-closo*-bimetallacarborane with a planar π-hydrocarbon ligand at the metal vertex.

The molecular structure of complex **8** is shown in Figure 3, and selected geometrical parameters (bond distances and angles) are listed in Table 3. The cage-bound methoxy group in **8** proved to be disordered over two positions, at the B(6) and B(3) atoms; both components, nevertheless, have been successfully modeled with a B(6):B(3) ratio of 80:20 in the X-ray diffraction experiment. On the basis of the X-ray diffraction study and multinuclear NMR spectra, both the **8a** and the **8b** isomers can be formally regarded as zwitterionic species, where the anionic icosahedral unit *closo*-{(η^6-C_6H_6)$RuC_2B_9H_{10}$(OMe)}$^-$ functions in a tridentate manner toward the incorporated cationic *exo*-{$RuCl(PPh_3)_2$}$^+$ fragment via three exopolyhedral B−H···Ru(1) bonds. In addition to the three H atoms of the boron cage, the *exo*-Ru(1) atom is bound to one Cl and two PPh_3 ligands, thus forming an octahedral coordination sphere. Of the three boron atoms participating in the three-bridge $(B-H)_3$···Ru(1) bonding system, one, namely B(11), belongs to the upper CB_4 belt of the cage, while the other two, B(10) and B(12), are from the adjacent pentagonal B_5 belt. The B−H−Ru(1) linkages are noticeably nonequivalent which is, apparently, due to the differences in the structural *trans* influence exerted by the PPh_3 and Cl ligands at the Ru(1) atom. As in all other known examples of three-bridge *exo-nido*- and *exo-closo*-metallacarborane complexes with {$MCl(PPh_3)_2$} (M = Ru or Os) units *exo* positioned to the cage ligand,[19,22] the shortest of the three Ru(1)−B bond distances in **8** lies *trans* to the Cl ligand (Ru(1)···B(12) = 2.270(5) Å). The other two Ru(1)···B(10) and Ru(1)···B(11) bond distances of 2.426(5) and 2.443(4) Å, respectively, proved to be much longer since they are both positioned *trans* to ruthenium-bound PPh_3 groups. It has been previously observed for complex **11**[22e] that one of the PPh_3 ligands at the *exo*-Ru atom (not the Cl ligand) is located in the position *anti* to the metal vertex of the cage framework. Exactly the same conformation is realized for both isomers of complex **8**, in contrast with many other related complexes of *exo-nido*-{$MCl(PPh_3)_2$}-metallacarboranes (M = Ru[19a,b] or Os[19c,d]) and *exo-closo*-{$RuCl(PPh_3)_2$}-metallacarboranes,[22a−d] where the Cl ligand was found to be lying either in the *anti* position with respect to the "extra-hydrogen" atom or in the metal vertex, respectively.

The rather unusual configuration observed in the crystals of **8** may have a steric explanation. It seems obvious that if the Cl ligand in the major isomer **8a** would have taken either of the two positions occupied by the phosphine ligands (i.e., through the rotational twisting of the *exo*-{$RuCl(PPh_3)_2$} group relative to the B(10)−B(11)−B(12) triangular face[22e]), the steric hindrances between the 6-MeO group and the phosphine substituent at the *exo*-Ru atom would have been

Table 3. Selected Bond Lengths (Å) and Angles (deg) for Complex **8**

Ru(1)−Cl(1)	2.400(1)	Ru(2)−B(7)	2.219(5)
Ru(1)−P(1)	2.296(1)	Ru(2)−B(11)	2.162(4)
Ru(1)−P(2)	2.280(1)	Ru(2)−C(14)	2.235(5)
Ru(1)−B(10)	2.426(5)	Ru(2)−C(15)	2.226(5)
Ru(1)−B(11)	2.443(4)	Ru(2)−C(16)	2.228(5)
Ru(1)−B(12)	2.270(5)	Ru(2)−C(17)	2.210(5)
Ru(1)−H(10)	2.07(5)	Ru(2)−C(18)	2.206(5)
Ru(1)−H(11)	1.96(5)	Ru(2)−C(19)	2.226(5)
Ru(1)−H(12)	1.82(5)	B(6)−O(1)	1.392(6)
Ru(2)−C(1)	2.179(5)	O(1)−C(13)	1.429(8)
Ru(2)−B(3)	2.202(5)	B(3)−O(1′)	1.31(2)
Ru(2)−B(6)	2.192(5)	O(1′)-C(13′)	1.44(3)
P(1)−Ru(1)−Cl(1)	96.02(4)	P(2)−Ru(1)−H(11)	91(1)
P(2)−Ru(1)−Cl(1)	96.69(4)	H(12)−Ru(1)−Cl(1)	171(1)
P(2)−Ru(1)−P(1)	97.95(4)	H(12)−Ru(1)−P(1)	90(1)
Cl(1)−Ru(1)−H(10)	84(1)	H(12)−Ru(1)−P(2)	88(1)
P(1)−Ru(1)−H(10)	90(1)	H(10)−Ru(1)−H(11)	81(2)
P(2)−Ru(1)−H(10)	172(1)	H(12)−Ru(1)−H(10)	90(2)
Cl(1)−Ru(1)−H(11)	84(1)	H(12)−Ru(1)−H(11)	89(2)
P(1)−Ru(1)−H(11)	171(1)	B(6)−O(1)−C(13)	119.7(4)
		B(3)−O(1′)−C(13′)	123(2)

(21) (a) Calabrese, J. C.; Fischer, M. B.; Gaines, D. F.; Lott, J. W. *J. Am. Chem. Soc*. **1974**, *96*, 6318. (b) Hildebrandt, D. F.; Gaines, D. F.; Calabrese, J. C. *Inorg. Chem.* **1978**, *17*, 790. (c) Elrington, M.; Greenwood, N. N.; Kennedy, J. D.; Thornton-Pett, M. *J. Chem. Soc., Dalton Trans.* **1987**, 451.

(22) (a) Chizhevsky, I. T.; Yanovsky, A. I.; Struchkov, Yu. T. *J. Organomet. Chem.* **1997**, *536*−*537*, 51 (short review). (b) Ellis, D. D.; Jelliss, P. A.; Stone, F. G. A. *Organometallics* **1999**, *18*, 4982. (c) Ellis, D. D.; Jelliss, P. A.; Stone, F. G. A. In *Contemporary Boron Chemistry*; Davidson, M. G., Hughes, A. K., Marder, T. B., Wade, K., Eds.; Royal Society of Chemistry: Cambridge, U.K., 2000; p 291. (d) Kolomnikova, G. D.; Sorokin, P. V.; Petrovskii, P. V.; Chizhevsky, I. T.; Barakovskaya, I. G.; Dolgushin, F. M.; Yanovsky, A. I. In *Contemporary Boron Chemistry*; Davidson, M. G., Hughes, A. K., Marder, T. B., Wade, K., Eds.; Royal Society of Chemistry: Cambridge, U.K., 2000; p 321. (e) Ellis, D. D.; Franken, A.; Jelliss, P. A.; Kautz, J. A.; Stone, F. G. A.; Yu, P.-Y. *J. Chem. Soc., Dalton Trans*. **2000**, 2509. (f) Du, S.; Kautz, J. A.; McGrath, T. D.; Stone, F. G. A. *Inorg. Chem.* **2001**, *40*, 6563.

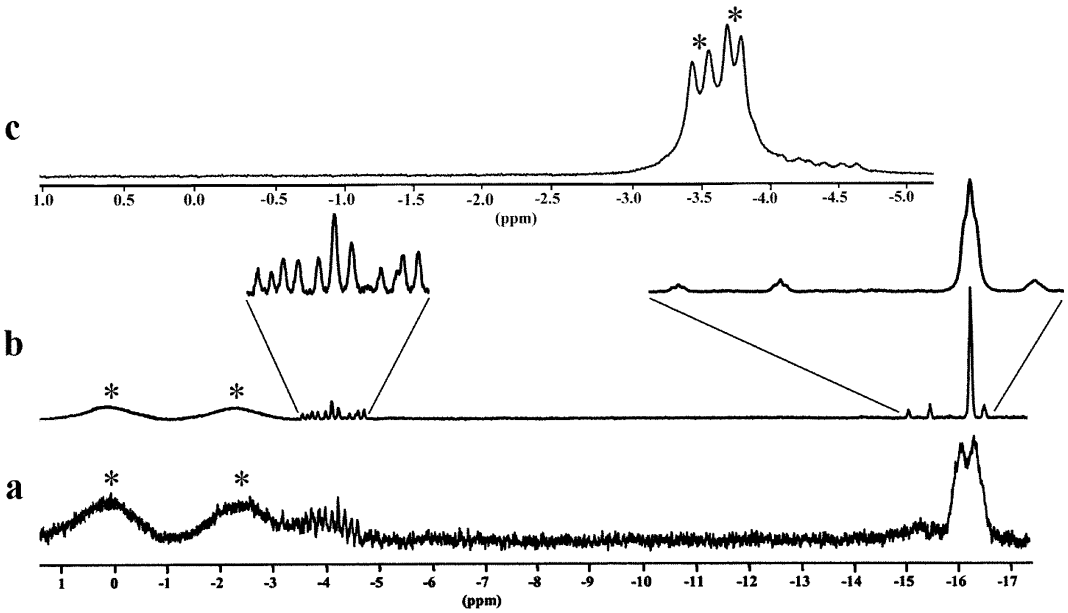

Figure 3. 400 MHz ^{1}H (a) and ^{1}H{^{11}B} (b) NMR spectra of **8a**,**b** in CD_2Cl_2 (hydride region) at 20 °C and 400 MHz ^{1}H{^{11}B} NMR spectrum of **8a**,**b** in CD_2Cl_2 at −83 °C (c), showing fully decoupled resonances of bridging hydrogens H(7) and H(11) of **8a** along with those of **8b** (weak overlapped peaks).

Chart 1. Schematic Representation of Dynamic Processes for Complexes **8a** and **8b** in Solution

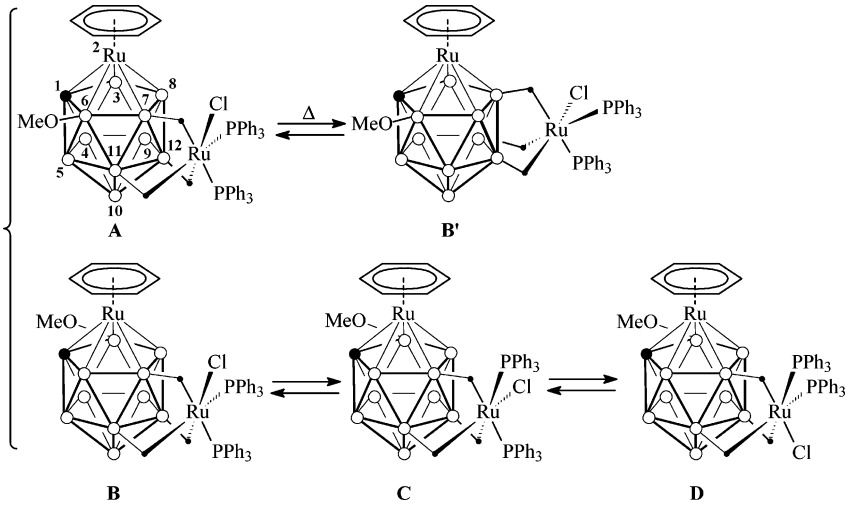

far more significant than in the existing structure. Therefore, it is reasonable to think that isomer **8a** in solution has the same conformation as that observed in the crystal state (Chart 1A). The *exo*-{RuCl(PPh$_3$)$_2$} fragment in the minor isomer **8b**, in contrast, happens to be much further away from the 3-MeO group of the carborane ligand; therefore, none of the three conceivable conformations depicted in Chart 1B−D should be ruled out as being sterically unfavorable. Interestingly, in isomer **8a**, the less sterically demanding geometry of the *exo*-{RuCl(PPh$_3$)$_2$} fragment could have been possible. Such a configuration can be theoretically attained by the transfer of the Ru atom toward the B(7)−B(8)−B(12) triangular face, which involves the second boron atom of the carborane CB_4 belt being in the β-position relative to a cage carbon. In this case, isomer **8b′** with this geometry (Chart 1B′) would, in fact, represent the enantiomer of **8b** (Chart 1B) and the diastereomer of **8a** (Chart 1A). The question that may arise from this consideration is why, in the crystal structure of **8**, does sterically hindered isomer **8a** predominate over isomer **8b**, where steric repulsion between the *exo*-{RuCl(PPh$_3$)$_2$} and the methoxy function is minimal. One of the possible explanations could be electronic reasons which imply that the electron-donor methoxy group promotes, by creating the highest negative charge on the neighboring cage boron atoms, a more effective transfer of electrons from the adjacent B−H bonds to the ruthenium atom in the formation of the (B−H)$_3$···Ru agostic system in **8a**. However, in this case, the crystal-packing effect might also be significant.

The results of the X-ray study and the qualitative conformational analyses presented above are in good agreement with the ^{1}H/^{1}H{^{11}B} and ^{31}P{^{1}H} NMR data obtained for **8**. Thus, in the fully boron-decoupled room-temperature ^{1}H-{^{11}B} NMR spectrum of **8** (Figure 3b), the high-field resonances corresponding to the B−H···Ru bridges for all three conformers of minor isomer **8b** (six weak doublets in the range between δ −3.6 and −4.7 ppm and three triplets at δ −15.00, −15.42, and −16.46 ppm) and the resonances

for the stable conformer of major isomer **8a** (two broad peaks centered at δ +0.23 and −2.27 ppm and the resonance at δ −16.19 ppm) are observed. The resonances found in the highest field of the spectrum, due to their triplet-like character and the low value of the $^2J(P_1,H) \sim {}^2J(P_2,H)$ coupling constants of ca. 8.5 Hz, were attributed to the B−H···Ru bridging hydrogens located *cis* to each of the PPh_3 ligands in both isomers **8a** and **8b**. As can be seen from Figure 3b, among the three B−H···Ru resonances found in this spectrum for **8a**, only the resonance at δ −16.19 (1H) ppm, which we attribute to the unique H(12) atom, reveals a triplet-like structure, whereas the other two signals centered at δ +0.23 (1H) and −2.27 (1H) ppm, and thus corresponding to bridging hydrogens in the *trans* position with respect to the PPh_3 groups, become fully decoupled only at temperatures down to −83 °C giving rise to two broad doublets at δ −3.49 and −3.74 ppm, each with a ^2J(H,P) value of ca. 45 Hz (Figure 3c). This phenomenon can be understood by realizing that at temperatures above −83 °C, the *exo*-{RuCl-$(PPh_3)_2$} fragment rapidly migrates between two adjacent cage triangular faces, B(10)−B(11)−B(12) and B(7)−B(8)−B(12) in structure **8a**, giving rise to the exchange of the two bridging hydrogens which lie *trans* to the PPh_3 ligands. Finally, such a migration process should result in the interconversion between diastereomers **8a** and **8b**, with the magnitude of K_{eq} determined by the differences in thermodynamic stabilities between these two species.

Next, we examined a series of variable-temperature $^{31}P\{^1H\}$ NMR spectra of **8** in d_8-THF in the range of −93 to +63 °C, which were also indicative of the fluxional behavior of this species in solution (Figure 4). The low-temperature $^{31}P\{^1H\}$ NMR spectra of **8**, in the range from −93 to −53 °C, consist of two principal resonances due to nonequivalent PPh_3 groups of major isomer **8a** with a chemical shift difference ($\Delta\nu$) of 4.9 ppm. In addition, a set of weak and partially overlapped resonances originating from the PPh_3 groups of conformationally fluxional isomer **8b** are seen in the spectrum. In the temperature range between −20 °C and room temperature, the spectra become more complex, displaying broad and unresolved resonances of both high and low intensities which could not be clearly interpreted. However, at the high-temperature limit (+63 °C), the spectrum simplifies again, exhibiting a pair of rather sharp doublets [^2J(P,P) = 35 Hz] with $\Delta\nu$ = 2.0 ppm along with weak resonances which were broadened and therefore almost unnoticed. The observation of the sharpening of two unique doublets of **8a** coupled with the broadening and even coalescence of some resonances of **8b** appears to be consistent with a relatively fast interconversion between **8a** and **8b** at the elevated temperature. On the basis of these data, one would also suggest that the rotational twisting processes in isomers **8a** and **8b** proceed at different rates on the NMR time scale.

Conclusion

In this paper, the synthesis of novel examples of *exo-closo*-arene-biruthenacarborane clusters of the general formulas [*closo*-2-(7,11-*exo*-$RuClPPh_3(\mu,\eta^6$-$C_6H_5PPh_2)$)-7,11-$(\mu$-$H)_2$-2,1-$RuCB_{10}H_8R$] (R = H, 6-MeO, or 3-MeO) and [*closo*-2-(η^6-C_6H_6)-10,11,12-(*exo*-$RuCl(PPh_3)_2$)-10,11,12-$(\mu$-$H)_3$-2,1-$RuCB_{10}H_7R^1$] (R^1 = 6-MeO or 3-MeO, an inseparable mixture of isomers) has been described in which the *nido*-$\{CB_{10}\}$ cage functions via two or three B−H···Ru bonds, respectively, as a bidentate or a tridentate ligand toward an exopolyhedral metal-containing moiety. Although in both types of complexes there are arene groups ligated by the *endo*-Ru atom, their nature and mode of function in each series are quite different. In the former complexes, the arene ligands are from one of the PPh_3 groups that is P-coordinated to the *exo*-Ru center, and therefore these are μ,η^6-bridging ligands. In the latter complexes, discrete arene ligands exhibit the well-recognized η^6-coordination mode with respect to the *endo*-Ru vertex. Unlike the complexes with bridging μ,η^6-arene ligands, the compounds with η^6-arene ligands undergo a distinct isomerization process through the scrambling of

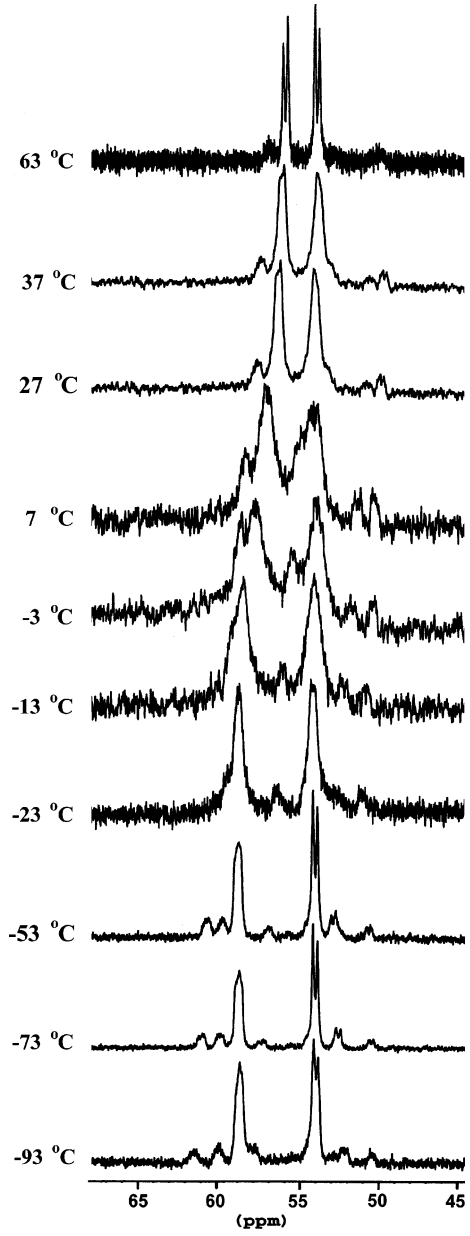

Figure 4. Variable-temperature $^{31}P\{^1H\}$ NMR spectra of isomers **8a**,**b** in d_8-THF solution in the range of −93 to +63 °C.

Table 4. Summary of Crystal Structure Determination Parameters for Compounds **6**−**8**

	6	**7**	**8**
formula	$C_{38}H_{43}B_{10}ClOP_2Ru_2$ 0.75(CH_2Cl_2)	$C_{38}H_{43}B_{10}ClOP_2Ru_2$ 2(CH_2Cl_2)	$C_{44}H_{49}B_{10}ClOP_2Ru_2$ 0.5(CH_2Cl_2) 0.5(CH_3OH)
mol wt	987.05	1093.21	1059.95
cryst syst	triclinic	triclinic	triclinic
space group	$P\bar{1}$	$P\bar{1}$	$P\bar{1}$
temperature (K)	120(1)	173(2)	153(2)
a (Å)	10.835(1)	13.806(7)	13.051(3)
b (Å)	17.871(2)	15.138(7)	13.417(4)
c (Å)	22.861(3)	24.143(10)	15.722(4)
α (deg)	68.881(3)	102.75(3)	81.75(2)
β (deg)	83.943(3)	98.86(4)	75.58(2)
γ (deg)	88.913(3)	99.43(4)	72.07(2)
V (Å^3)	4105.6(8)	4759(4)	2530(1)
Z	4	4	2
d_{calc} (g/cm^3)	1.597	1.526	1.391
μ (Mo Kα, λ = 0.71073 Å) (cm^{-1})	10.10	10.15	8.00
diffractometer	SMART CCD 1000	Siemens P3/PC	Siemens P3/PC
reflns collected	43331	16958	12723
independent reflns (R_{int})	19801 (0.0669)	16202 (0.0321)	12202 (0.0202)
observed reflns ($I > 2\sigma(I)$)	9116	13209	10245
R1[a]	0.0534	0.0544	0.0545
wR2[b]	0.1122	0.1279	0.1440

[a] $R1 = \sum||F_o| - |F_c||/\sum|F_o|$. [b] $wR2 = \{\sum[w(F_o^2 - F_c^2)^2]/\sum w(F_o^2)^2\}^{1/2}$.

the *exo*-{$RuCl(PPh_3)_2$}$^+$ fragment about two adjacent triangular boron faces, B(7)B(11)B(12) and B(8)B(9)B(12), which are located *trans* to a cage carbon atom, and this can be observed by variable-temperature $^1H\{^{11}B\}$ and $^{31}P\{^1H\}$ NMR spectroscopy.

Experimental Section

General Considerations. The reaction described above was carried out using standard Schlenk equipment under an atmosphere of dry argon. All solvents, including those used for column chromatography as eluents, were dried under appropriate drying agents and distilled under argon prior to use. The starting materials of [$RuCl_2(PPh_3)_3$] (**1**)[23] and [Cs][*nido*-7-$CB_{10}H_{13}$] (**2**)[24] were prepared according to literature methods. All room- and low-temperature NMR spectra were obtained with a Bruker AMX-400 spectrometer (^1H, 400.13 MHz; ^{31}P, 161.98 MHz; ^{11}B, 128.33 MHz) using TMS as an internal reference and 85% H_3PO_4 and $BF_3{\cdot}Et_2O$ as the external references, respectively. IR spectra were obtained from KBr pellets on a Specord M-82 instrument. Microanalyses were performed by the Analytical Laboratory of the Institute of Organoelement Compounds of the Russian Academy of Sciences.

Reaction of $RuCl_2(PPh_3)_3$ (1) with [Cs][*nido*-7-$CB_{10}H_{13}$] (2) in the Presence of tmnd. To a solution of **2** (0.15 g, 0.78 mmol) in 5 mL of degassed MeOH was added tmnd (0.33 g, 1.56 mmol), and after the resulting mixture was stirred for 30 min at room temperature, a solution of **1** (1.5 g, 1 mmol) in 60 mL of a 1:1 mixture of C_6H_6/MeOH was added dropwise. The solution was stirred at ambient temperature for 1 h and then was refluxed for 4 h. After the mixture was cooled, the solvent was evaporated to dryness under reduced pressure, and the residue was treated by column chromatography on silica gel (70−230 mesh) eluting a red band, composed of a mixture of **5**, **7**, and **9** with CH_2Cl_2. A second red band composed of a mixture of **6**, **8**, and **10** was then eluted with a 3:1 mixture of C_6H_6/Et_2O. Each of the fractions obtained was finally separated into individual compounds by repeated column chromatography on 230−400 mesh silica gel using the same solvents as eluents. The compounds from both fractions were collected with yields as follows: **5** (R_f = 0.85, 36 mg (5%)), **6** (R_f = 0.21, 57 mg (8%)), **7** (R_f = 0.71, 125 mg (17%)), **8** (R_f = 0.55, 71 mg (9%)), **9** (R_f = 0.76, 15 mg (1.2%)), and **10** (R_f = 0.48, 22 mg (1.7%)). IR spectroscopic and analytical data for complexes **5**−**7** follow (multinuclear NMR data of **5**−**7** are listed in Table 1). For **5**, the data follow. IR ν_{BH}: 2540 cm^{-1}. Anal. Calcd for $C_{37}H_{41}B_{10}ClP_2Ru_2$: C, 49.74; H, 4.63; B, 12.10; Cl, 3.97. Found: C, 49.76; H, 4.95; B, 11.35; Cl, 3.90. For **6**, the data follow. IR ν_{BH}: 2536 cm^{-1}. Anal. Calcd for $C_{38}H_{43}B_{10}ClOP_2Ru_2$: C, 49.43; H, 4.69; B, 11.71; Cl, 3.84. Found: C, 49.51; H, 4.75; B, 11.66; Cl, 3.69. For **7**, the data follow. IR ν_{BH}: 2540 cm^{-1}. Anal. Calcd for $C_{38}H_{43}B_{10}ClOP_2Ru_2$: C, 49.43; H, 4.69; B, 11.71. Found: C, 49.47; H, 4.82; B, 11.43. Characterization data of **8** follow. IR ν_{BH}: 2546 cm^{-1}. $^1H\{^{11}B\}$ NMR (CD_2Cl_2, 22 °C; the asterisk indicates nonoverlapping signals of fluxional isomer **8b** composed of three conformers (see Chart1B−D) of ca. 2.5:1.75:1 relative intensities): δ 7.39−7.10 (m, 30H, PPh_3), 5.81*, 5.78*, 5.50* (each s, 6H, C_6H_6), 5.52 (s, 6H, C_6H_6), 3.29*, 3.17 (each s, 1H, CH_{Cb}), 3.27 (s, 3H, MeO), 2.56, 1.97, 1.7−1.3 (2 × s br + m, BH), 0.23, −2.27 (each s br, 1H, B−H···Ru), −3.62*, −3.81*, −4.06*, −4.19*, −4.57*, −4.68* (each d br, 1H, ^2J(H,P) ∼ 44 Hz, B−H···Ru), −15.00*, −15.42*, −16.46* (each t br, 1H, ^2J(H,P) ∼ 8.5 Hz, B−H−Ru), −16.19 (t br, 1H, ^2J(H,P) = 8.2 Hz, B−H(12)···Ru). $^{31}P\{^1H\}$ NMR (d_8-THF, J(P,P), −73 °C; the asterisk indicates ^{31}P chemical shifts of fluxional isomer **8b**): δ 60.9* (s br), 59.7* (d br, 59), 58.6 (s br), 57.1* (d br, 42), 54.3* (partly overlapped), 53.7 (d, 46), 52.2* (d br, 52), 50.2* (d br, 40). Anal. Calcd for $C_{44}H_{49}B_{10}ClOP_2Ru_2{\cdot}CH_2Cl_2$: C, 50.30; H, 4.68; B, 9.95. Found: C, 50.56; H, 4.83; B, 9.97.

Crystal Data Collection and Structure Refinement Parameters for Complexes 6−8. X-ray quality crystals of **6**−**8** were grown by slow crystallization of samples from a CH_2Cl_2 *n*-hexane solution. Details of the data collection and structure refinement of compounds **6**−**8** are presented in Table 4. Data were corrected for Lorentz and polarization effects. An absorption correction for compound **6** was carried out according to the SADABS procedure.[25] The single-crystal samples of **7** and **8** were carefully chosen, well formed, and essentially isometric, and the quality of the obtained

(23) Stephenson, T. A.; Wilkinson, G. *J. Inorg. Nucl. Chem.* **1966**, *28*, 945.
(24) Knoth, W. H.; Little, J. J.; Lawrence, J. R.; Scholer, J. R.; Todd, L. J. *Inorg. Synth.* **1968**, *11*, 33.

results and the relatively low absorption coefficient values justified no need for absorption corrections. All of the structures have been solved by direct methods and refined by the full-matrix least-squares procedure in anisotropic approximation for non-hydrogen atoms. All of the hydrogen atoms in the carborane cages of molecules **6**−**8** were located in the difference Fourier maps and refined in the riding motion approximation (for **6**) and isotropic approximation (for **7** and **8**). The remaining hydrogen atoms in structures **6**−**8** were placed geometrically and included in the structure factor calculations in the riding motion approximation. The SHELXTL-97 program [26] was used throughout the calculations.

(25) Sheldrick, G. M. *SADABS: Program for Empirical Absorption Correction of Area Detector Data*; University of Göttingen: Göttingen, Germany, 1996.
(26) Sheldrick, G. M. *SHELXTL-97*, version 5.10; Bruker AXS Inc.: Madison, WI, 1997.

Acknowledgment. The authors gratefully acknowledge the financial support of the Russian Foundation for Basic Research (Grant 03-03-32651), the Program of Basic Research of the Chemistry and Materials Science Division of the Russian Academy of Sciences (Project 591-07), and the Leading Schools of the President of the Russian Federation LS-1060.2003.03.

Supporting Information Available: Complete tables of crystallographic data for structures **6**−**8**, as well as data in CIF format. Tabulated data of selective proton decoupling experiment for complex **5**. This material is available free of charge via the Internet at http://pubs.acs.org.

IC0497883